Journal of Magnetism and Magnetic Materials 323 (2011) 2196–2201

Contents lists available at ScienceDirect

Journal of Magnetism and Magnetic Materials

journal homepage: www.elsevier.com/locate/jmmm

Step-shape angular spin distribution in layered systems by ^{57}Fe Mössbauer spectroscopy: A general treatment

V. Kuncser [a,*], W. Keune [b,c]

[a] National Institute of Materials Physics, P.O. Box MG 7, 077125 Magurele-Bucharest, Romania
[b] Fakultät für Physik, Universität Duisburg-Essen, D-47048 Duisburg, Germany
[c] Max-Planck-Institut für Mikrostrukturphysik, D-06120 Halle, Germany

ARTICLE INFO

Article history:
Received 24 February 2011
Available online 1 April 2011

Keywords:
Angular spin distribution
Mössbauer spectroscopy
^{57}Fe

ABSTRACT

In the so-called 'step-shape' angular spin distribution model for layered systems, the non-collinear directions of the atomic magnetic moments are confined to the film plane and form a homogeneous fan spanning inside an (in-plane) angular interval $\Delta\varphi$ centered at an angle φ_0. A general approach for deriving the two parameters φ_0 and $\Delta\varphi$ via ^{57}Fe Mössbauer spectroscopy measurements is discussed. The analysis extends our previously reported treatment, which assumed that the angular aperture $\Delta\varphi$ develops symmetrically versus a fixed direction φ_0 (e.g., the in-plane easy axis of magnetization) oriented either along or perpendicular to the in-plane projection of the Mössbauer γ-ray direction. The proposed approach is also applicable for those cases when not only the spin aperture $\Delta\varphi$ is changing but also the aperture center φ_0 is rotating under the influence of different external parameters, such as applied field, temperature, stress, etc. The method is suitable for applications to nanoscale layered heterostructures with in-plane uniaxial or unidirectional magnetic anisotropy. The method is applied to experimental data obtained on a 2-nm thick defected Fe layer with in-plane magnetic texture.

1. Introduction

Many interesting magnetic phenomena in thin films and multilayers are strongly dependent on the involved spin configurations. The spin structure at the interface of hard–soft ferromagnetic layers or at ferromagnetic–antiferromagnetic layers is a key factor in explaining exchange-spring [1,2] or exchange-bias [3,4] phenomena, respectively, whereas spin-dependent electron scattering is intimately related to the spin structure at the interface between a magnetic and a non-magnetic conductive layer [5,6]. In such nanoscale layered heterostructures non-collinear spiral-like magnetic structures may evolve in the interfacial regions under the action of external parameters, e.g., applied magnetic fields. The experimental determination of the spin structure by different methods (like, e.g., polarized neutron reflectometry [7], X-ray resonant magnetic scattering [8], nuclear resonant X-ray scattering [9–11], and Mössbauer spectroscopy [2,4,12]) is a challenge and requires useful models for data interpretation. ^{57}Fe Mössbauer spectroscopy, being isotope selective, is one of the most powerful techniques for a comprehensive study of structural and electronic properties, including magnetic interactions and spin structures, in different materials. The interfacial spin configuration as well as the depth-dependent spin distributions in Fe containing layered systems can be measured via conversion electron Mössbauer spectroscopy (CEMS) using tracer layers enriched in the ^{57}Fe isotope, placed either at the interface or at a certain distance from the interface [2,4,12].

A practical approach to characterize the in-plane angular Fe spin distribution in layered systems, via different Mössbauer spectroscopy geometries, was proposed in Refs. [13,14]. The experiment should be performed with the Mössbauer γ-ray incident under a certain angle $\phi \neq 90^\circ$, relative to the film surface (see Fig. 1) because of reasons given in Section 2. In a magnetically ordered material, a sufficiently large hyperfine magnetic field, B_{hf}, at the ^{57}Fe nucleus leads to a Zeeman splitting of the Mössbauer spectrum exhibiting the well-known six lines. The direction of the hyperfine magnetic field, B_{hf}, is known to be antiparallel to the direction of the magnetic moment, μ_{Fe}, of the ^{57}Fe atom, i.e., B_{hf} and μ_{Fe} are collinear. Therefore, the angular distribution of B_{hf} is equivalent to the angular distribution of μ_{Fe}. The intensity ratio, R_{23}, of the Mössbauer-sextet lines #2 and 3 (or, equivalently, lines #5 and 4, counted from left to right) is a measure of the average Fe spin direction (relative to the incident Mössbauer γ-ray direction) in the sample. The R_{23} ratio is usually obtained by least-squares fitting the measured Mössbauer spectra. The experimental R_{23} ratio can be theoretically expressed in terms of the parameters of modeled angular Fe spin distributions. Finally, the most appropriate distribution parameters are obtained by minimizing the

* Corresponding author. Tel.: +4021 369 01 85; fax: +4021 369 01 77.
E-mail address: kuncser@infim.ro (V. Kuncser).

0304-8853/$ - see front matter © 2011 Elsevier B.V. All rights reserved.
doi:10.1016/j.jmmm.2011.03.030

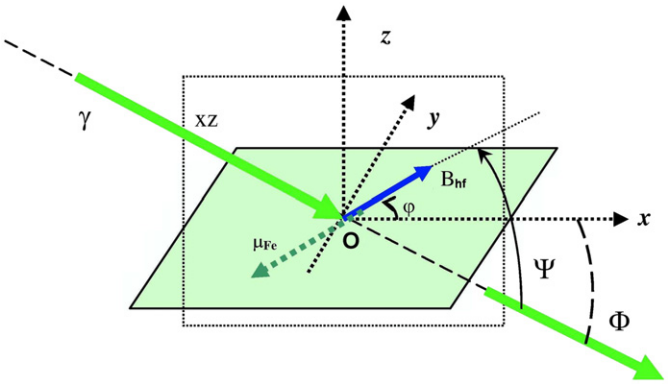

Fig. 1. A Mössbauer experiment in non-perpendicular geometry, suitable for characterization of the in-plane angular distribution of the hyperfine magnetic field B_{hf} and of the Fe magnetic moment μ_{Fe}. Ψ is the angle between B_{hf} (or μ_{Fe}) and incident γ-ray direction and Φ is the angle between γ-ray direction and the sample plane (or x axis). The sample plane is the xy plane.

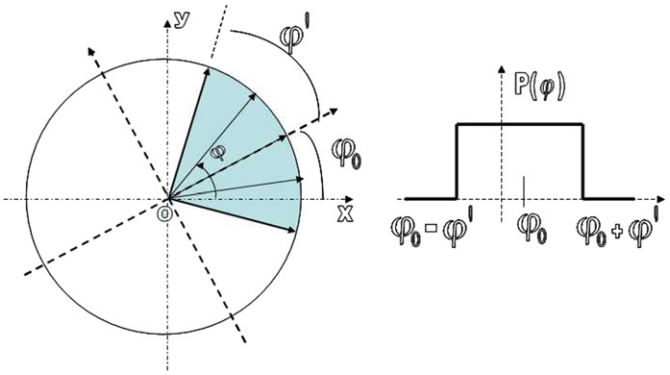

Fig. 2. A schematic representation of the Fe spins in the sample plane (xy plane, left) in case of an angular step-shape distribution (right). The discussion will concentrate on the angle φ_0 of the aperture center with respect to the Ox axis in Fig. 1, and on the aperture $\Delta\varphi=2\varphi'$.

difference between theoretical and experimental R_{23} ratios. In this context, a convenient and realistic type of angular Fe spin distribution should be initially assumed in order to describe the experimental data. This means that the method works well if one has an idea about the real angular spin distribution in the sample, e.g., if the Fe spins are distributed about a known preferential magnetic direction in the sample. However, if the assumed angular distribution is far away from the real one, the theoretical data cannot reproduce the experimental dependencies well enough and another type of distribution has to be assumed.

A lot of work concerning the study of the spin texture by Mössbauer spectroscopy was reported during the last decades [13–24]. In fact, there are two types of approaches for the experimental characterization of the spin texture by this method. The most complete theory, presented by Pfannes and Fischer [15], describes the spin texture by a two-variable probability density function $D(\theta,\varphi)$, with θ and φ being the polar and azimuthal angles, respectively, of the quantization axis of the ^{57}Fe nucleus versus a fixed laboratory system. When working with unpolarized radiation, this function can be reasonably approximated via a set of five coefficients related to its expansion in spherical harmonics. However, in spite of its generality, this theory could not be easily applied in experiments. Therefore, later Greneche and Varret [16] have introduced simplifications, showing that a spin texture of D_{2h} symmetry (e.g., an ellipsoidal representation of the probability distribution) can be adequately described by only two independent parameters. This simplified model, assuming *a priori* a three-dimensional ellipsoidal type of angular spin distribution, was frequently applied, for instance in Refs. [17–23]. The possibility of measuring spin texture independent Mössbauer spectra by the 'magic-angle' method is also implied [23]. A review of the available versions of the spin texture models, with applications to the case of 3d-based (ribbon-like) amorphous ferromagnets, was given by Pankhurst and Gibbs [24], who emphasized also the limits of the model by Greneche and Varret. Furthermore, the sharpened interest in magnetic phenomena of thin films and multilayers imposed the development of specific procedures for the evaluation of Mössbauer data in case of angular spin distributions in layered systems with in-plane magnetic shape anisotropy, where the magnetic moments are oriented in the film plane and the spin texture is reduced to two dimensions. In-plane magnetic anisotropy is the most frequently occurring case in thin film/multilayer systems. For such a situation, we recently proposed a new and simplified approach [13,14], the so-called step-shape angular spin distribution model (see below), which was critically discussed with respect to previous models by pointing out both its advantages and limitations [13]. The requirement for assuming an in-plane angular spin distribution function for two-dimensional systems represents, on one hand, a strong limitation of our model, but on the other hand avoids further considerations on the intrinsic system symmetry. Different applications of this model have been provided [2,4,11–14], most often by solving numerically the relationship between the experimental R_{23} ratio and the angular spin distribution parameters, specific to various types of assumed distribution functions.

The aim of the present work is to provide a general analytic expression for the intensity ratio R_{23} as a function of the two typical parameters of the step-shape angular distribution of Fe spins with directions confined to the film plane. In this model the Fe magnetic moment directions form a homogeneous fan-like arrangement spanning an (in-plane) angular interval $\Delta\varphi$ $(=2\varphi')$ centered at an angle φ_0 (see Fig. 2). The two parameters to be determined from the experimental R_{23} ratio are $\Delta\varphi$ $(=2\varphi')$ and φ_0. This distribution is considered as one of the most convenient model distributions, which is simple but also realistic enough for a suitable simulation of a real in-plane angular spin distribution in layered systems [2,12]. Particular expressions for special cases, reported in Ref. [14], are regained, and the conditions of their viability are discussed. Finally, the method is applied to the case of a 2-nm thick defected Fe film that exhibits in-plane magnetic texture.

2. Experimental geometry and theory

The geometry of the experiment is the one reported in Ref. [13] (see also Fig. 1). The thin film lies in the xy plane and the γ-ray is incident onto the sample plane under an angle ϕ (relative to the Ox axis, in the Oxz plane). The magnetic hyperfine field, B_{hf} (a typical Mössbauer parameter whose magnitude is inferred from the Zeeman splitting in the spectra), is a vector quantity that is oriented in the sample plane and is antiparallel to the Fe atomic magnetic moment, and, hence, parallel to the Fe spin, and makes an angle φ with the Ox axis and an angle ψ with the direction of the γ-ray. For a unique direction Ψ of the magnetic hyperfine field with respect to the γ-ray direction, the intensity ratio R_{23} of the second (I_2) to the third (I_3) line of the Mössbauer sextet is defined as $R_{23}=I_2/I_3=4\sin^2(\psi)/[1+\cos^2(\psi)]$ (likewise, one can define the ratio $R_{54}=R_{23}=I_5/I_4$ as the intensity ratio of the fifth (I_5) to the fourth (I_4) line of the sextet). In case of an angular spin distribution $P(\psi)$, both intensities I_2 and I_3 and, hence, $\sin^2(\psi)$ as well as $[1+\cos^2(\psi)]$ should be averaged over all possible spin orientations. The

following expression is obtained for the intensity ratio R_{23} [14]:

$$R_{23} = 4\frac{\int_\psi \sin^2(\psi)P(\psi)d\psi}{1+\int_\psi \cos^2(\psi)P(\psi)d\psi} \quad \text{with} \int_\psi P(\psi)d\psi = 1 \tag{1}$$

When dealing with an in-plane angular spin distribution, more convenient angular parameter φ (Fig. 1) and the probability distribution $P(\varphi)$ can be chosen, under the condition that $P(\varphi)\mathrm{d}\varphi = P(\psi)\mathrm{d}\psi$ [13]. Using the angle of γ-ray incidence ϕ and introducing also the relationship $\cos(\psi)=\cos(\phi)\cos(\varphi)$, which can be straightforwardly derived by analytical geometry [13], the R_{23} ratio can be generally expressed as [14]

$$R_{23} = 4\frac{1-\cos^2(\phi)\langle\cos^2(\varphi)\rangle}{1+\cos^2(\phi)\langle\cos^2(\varphi)\rangle} \tag{2}$$

with

$$\langle\cos^2(\varphi)\rangle = \int_0^{2\pi}\cos^2(\varphi)P(\varphi)\mathrm{d}\varphi \quad \text{and} \quad \int_0^{2\pi}P(\varphi)\mathrm{d}\varphi = 1$$

Eq. (2) demonstrates that $R_{23}=4$ for perpendicular γ-ray incidence, i.e., for $\phi=90^\circ$, and in this case R_{23} becomes insensitive to the in-plane spin orientation. Eq. (2) will be applied for a step-shape angular spin distribution as a model. It is worth mentioning that due to the parallel (antiparallel) orientation of the magnetic hyperfine field and the Fe spin (Fe magnetic moment), a full characterization of the angular probability distribution of the magnetic hyperfine field is equivalent to the characterization of both the angular spin distribution and the angular magnetic moment distribution.

By a step-shape angular distribution one understands that the hyperfine fields (or Fe spins) are pointing with the same probability into an angular aperture $\Delta\varphi=2\varphi'$, centered at the angle φ_0 with respect to the *Ox* axis. Graphically, this situation can be represented by hyperfine fields (or spins) pointing with the same density (number of spins per unit angle) along different angles inside the interval $\Delta\varphi=2\varphi'$ (Fig. 2). Mathematically, the distribution probability for this case can be expressed as follows: $P(\varphi)=P_0$ for $\varphi_0-\varphi' \le \varphi \le \varphi_0+\varphi'$, and $P(\varphi)=0$ in the rest of the 2π interval. Hence

$$\langle\cos^2(\varphi)\rangle = \int_0^{2\pi}\cos^2(\varphi)P(\varphi)\mathrm{d}\varphi = P_0\int_{\varphi_0-\varphi'}^{\varphi_0+\varphi'}\cos^2(\varphi)\mathrm{d}\varphi \tag{3}$$

with $P_0=(1/2\varphi')=\text{constant}$, through the normalization condition for the probability distribution. Therefore, in case of the step-shape angular distribution of the spins, the solution of Eq. (2) is reduced to solving the simple integral $I=\int_{\varphi_0-\varphi'}^{\varphi_0+\varphi'}\cos^2(\varphi)\mathrm{d}\varphi$.

Integration leads to the expression:

$$2I = \varphi\big|_{\varphi_0-\varphi'}^{\varphi_0+\varphi'} + \sin(\varphi)\cos(\varphi)\big|_{\varphi_0-\varphi'}^{\varphi_0+\varphi'}$$

The following relationship is finally obtained via usual trigonometric relations:

$$\langle\cos^2(\varphi)\rangle = \frac{1}{2}+\frac{1}{2}\frac{\sin(2\varphi')}{2\varphi'}\cos(2\varphi_0) \tag{4}$$

Eq. (4) in combination with Eq. (2) is the general expression for the intensity ratio R_{23} in the frame of the step-shape angular spin distribution. However, the intensity ratio in this model depends on only two parameters (φ' and φ_0), which can be obtained from at least two Mössbauer experiments performed by rotating the sample in its own plane, i.e., by the azimuth angle φ around the *z* axis. Then, the experimental φ-dependence of R_{23} can be compared with the theoretical $R_{23}(\varphi)$ ratio according to Eq. (4) in order to extract the parameters φ' and φ_0. It is worth mentioning that the simplest case corresponds to the situation when the center φ_0 of the angular distribution is known (many practical situations fulfill this requirement, e.g., the center corresponds to the direction of the easy axis of magnetization, which can be established via complementary magnetic or structural measurements). In that case, the center of the angular distribution can be oriented either along ($\varphi_0=0^\circ$) or perpendicular ($\varphi_0=90^\circ$) to the in-plane projection of the γ-ray direction, i.e., to the *x* axis. Under these circumstances, $\langle\cos^2(\varphi)\rangle$ given by Eq. (4), becomes

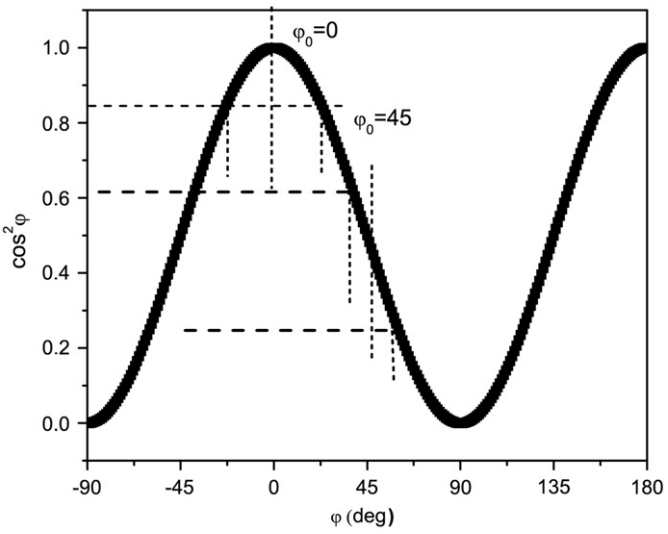

Fig. 3. Function $\cos^2(\varphi)$ vs. φ and its symmetry peculiarities for $\varphi_0=0^\circ$ and 45°.

$$\langle\cos^2(\varphi)\rangle = \frac{1}{2}\pm\frac{1}{2}\frac{\sin(2\varphi')}{2\varphi'} \tag{5}$$

which is identical to Eq. (6′) in Ref. [14], specialized for $\varphi_0=0^\circ$ or 90°. For $\varphi'\to 0^\circ$, Eq. (5) leads to $\langle\cos^2(\varphi)\rangle=1$ or 0 depending on $\varphi_0=0^\circ$ or 90°, in agreement with the unidirectional spin distribution model [14]. In order to discuss the differences between the most general Eq. (4) in this report and the special form of Eq. (6′) in Ref. [14], a reminder on the functional behavior of $\cos^2(\varphi)$ is helpful. It can be directly observed from Fig. 3 that for $\varphi_0=0^\circ$, $\cos^2(\varphi_0-\varphi')=\cos^2(\varphi_0+\varphi')$, whereas for $\varphi_0=45^\circ$, $\cos^2(\varphi_0-\varphi')\neq\cos^2(\varphi_0+\varphi')$. Eq. (6′) in Ref. [14] deals only with the case $\cos^2(\varphi_0-\varphi')=\cos^2(\varphi_0+\varphi')$, which allows to express the integral from $\varphi_0-\varphi'$ to $\varphi_0+\varphi'$ as twice the integral from φ_0 to $\varphi_0+\varphi'$. Eq. (4) in this report does not assume any condition on the function $\cos^2(\varphi)$ and φ_0 and, therefore, is more general.

3. Experimental confirmation and discussion

The practical application of Eq. (2) with $\langle\cos^2(\varphi)\rangle$ expressed by Eq. (4) involves two different approaches: (i) either the angular spin distribution is constant, being an intrinsic magnetic property of the material, or (ii) the angular spin distribution is uniformly modified under the influence of an external factor (e.g. an applied magnetic field).

The first case (i), which is typically met in layered systems with an angular distribution of the magnetic easy axes [25], assumes again two different situations: (a) the center of the angular distribution (φ_0) is well known with respect to a macroscopic direction in the sample plane or (b) the center of the angular distribution is not known with respect to such a macroscopic direction. In case (a), the only remaining parameter to be measured by Mössbauer spectroscopy is the semi-aperture φ'. This can be derived principally by a single Mössbauer measurement with the sample oriented with the center of the angular distribution at either $\varphi_0=0^\circ$ or 90° with respect to the projection of the γ-ray direction onto the sample plane and the subsequent

use of Eqs. (2) and (5). A more reliable value for φ' can be obtained by performing both experiments at $\varphi_0=0^\circ$ and 90° and fitting the measured difference $\Delta R_{23}=R_{23}(\varphi_0=90^\circ)-R_{23}(\varphi_0=0^\circ)$ to the difference between the two theoretical curves $R_{23}(\varphi')$ calculated for $\varphi_0=0^\circ$ and 90°, respectively, according to the same Eqs. (2) and (5) (see also the inset of Fig. 4).

The more complex case (b) can be elegantly solved via a series of Mössbauer measurements taken by rotating the sample in its own plane (i.e., around the z axis) and representing the R_{23} ratio for different angles between a marked direction in the sample plane and the in-plane projection of the γ-ray direction (Ox axis). Fig. 4 presents the theoretical dependencies of the intensity ratio R_{23} on the angle φ_0 (angle between the center of the distribution and the in-plane projection of the γ-ray direction) for different semi-apertures, φ'. One may notice in Fig. 4 that the amplitude of the oscillation depends strongly on the angular semi-aperture φ'. For $\varphi'<90^\circ$, the amplitude of the $R_{23}(\varphi_0)$ dependence decreases drastically with increasing φ' and becomes zero at $\varphi'=90^\circ$. The positions of the minimum (at $\varphi_0=0^\circ$) and maximum (at $\varphi_0=90^\circ$) are independent of φ'. For $90^\circ<\varphi'<180^\circ$, a maximum value of R_{23} is obtained at $\varphi_0=0^\circ$ and a minimum value at $\varphi_0=90^\circ$ (Fig. 4). However, the amplitude of the $R_{23}(\varphi_0)$ dependence is much lower than that for the case of $\varphi'<90^\circ$, reaching a broad maximum at $\varphi'=135^\circ$ and $\varphi_0=0^\circ$ (see also the inset of Fig. 4). Most of the interesting practical situations involve relatively narrow angular spin distributions, with $\varphi'<90^\circ$, and, hence, a fairly precise determination of both φ_0 and φ' can be provided by the representation proposed above for the experimental $R_{23}(\varphi)$ data. Obviously, according to Fig. 4, such a representation will show an oscillating behavior, with the maximum centered at $\varphi_0=90^\circ$ and the minimum at $\varphi_0=0^\circ$. The angular shift from $\varphi=90^\circ$ ($\varphi=0^\circ$) of the maximum (minimum) in the oscillating experimental $R_{23}(\varphi)$ data provides the orientation of the center of the angular distribution with respect to the direction marked on the sample, whereas the amplitude of the oscillation provides the value of the semi-aperture φ'.

In the following we present a practical example for the proposed procedure. We study the magnetic texture in a sample consisting of a polycrystalline thin film of Fe grown on a polycrystalline Cu buffer layer that covered a Si(0 0 1) wafer as a substrate. The native Si oxide was not removed. The substrate was cut with the edge along its [1 1 0] direction. The Fe film was protected by a thin Cu cap layer. The sample was prepared by rf sputtering in Ar (10^{-2} mbar) at a power of 100 W, with the substrate held at room temperature. The thickness of the Cu buffer layer (Cu cap layer) was 5 nm (2 nm), whereas the thickness of the Fe layer (partially enriched in the ^{57}Fe Mössbauer isotope) was about 2 nm. Since only one sputtering target could be incorporated in the rf sputtering chamber, the film deposition procedure involved opening of the chamber and exposure to air for a few minutes after deposition of each layer during the exchange of the Cu and Fe targets. However, this procedure did not cause significant oxidation of the Fe layer, since the CEM spectra on the sample (see below) did not reveal magnetic hyperfine field components larger than 45 T, which are typical for Fe oxides. X-ray diffraction provided evidence of a weak crystallographic texture in the Cu layers along [1 1 0] of the Si(0 0 1) substrate. This was confirmed for numerous other samples prepared in the same way. A mark was made at a low angle with respect to the [1 1 0] direction of Si(0 0 1), and the sample was initially magnetized along the [1 1 0] direction.

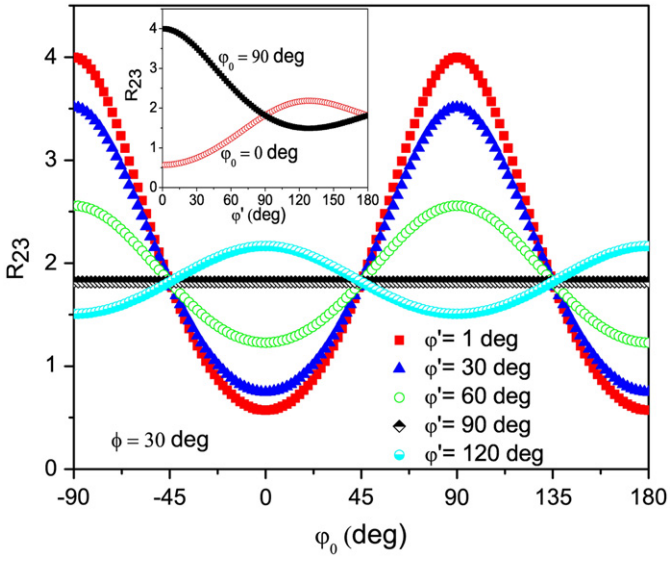

Fig. 4. Theoretical intensity ratio R_{23} vs. angle φ_0 for different semi-apertures φ'. An angle ϕ of 30° between the direction of the γ-ray and the sample plane was considered. The inset shows the $R_{23}(\varphi')$ dependence for $\varphi_0=0^\circ$ and 90°.

CEM spectra were acquired at room temperature in zero external field with the incident γ-radiation making an angle of $\varphi=50^\circ$ with the sample plane. Thus, the sample was at magnetic remanence during the measurements. The escape depth of the detected conversion electrons is about 100 nm [26], which covers far more than the depth and the thickness of the ^{57}Fe layer. The spectra were obtained at different angles φ between the mark and the projection of the γ-ray direction onto the sample plane (Ox direction). An additional spectrum was acquired in perpendicular geometry (at $\phi=90^\circ$). The spectra were least-squares fitted using the program NORMOS by Brand [27]. All these spectra are presented in Fig. 5.

The Mössbauer spectrum collected in perpendicular geometry (Fig. 5(a)) consists of a Zeeman-split sextet with very broad lines, providing evidence of strong interfacial diffusion of Cu atoms into the lattice of the Fe film. Thus, a Fe-rich disordered Fe–Cu alloy (i.e., Fe(Cu)) film is formed. Therefore, all the spectra were least-squares fit via a distribution $P(B_{hf})$ of magnetic hyperfine fields B_{hf} ($P(B_{hf})$ distributions are shown on the right hand side of Fig. 5). $P(B_{hf})$ is centered at an average B_{hf} value of about 31 T. This value is smaller than that of pure bulk bcc Fe ($B_{hf}=33.0$ T at room temperature) due to the influence of the impurity Cu neighboring atoms in the Fe lattice. The intensity ratio, R_{23}, obtained in perpendicular geometry is 3.9(1), proving the complete in-plane orientation of the Fe spins. The in-plane spin-orientation was also confirmed by magneto-optical Kerr effect (MOKE) measurements (see below). All the other spectra obtained at $\phi=50^\circ$ and $\varphi=-30^\circ$, 0°, 30°, 60° and 90° (Fig. 5(b), (c), (d), (e) and (f), respectively) show a similar shape and $P(B_{hf})$ distribution, but exhibit a clear variation in the R_{23} ratio. The as-shown distributions $P(B_{hf})$ deviate slightly from the reference distribution $P(B_{hf})$ at perpendicular geometry (Fig. 5(a)), especially in the range of low hyperfine fields (≤ 20 T) with low probability density, where mathematical oscillations might mask the physically relevant low-field distribution tail. The ratios of the absolute area of such deviations and the area of the reference distribution are less than 10% (with the main deviation appearing in the low-field range). We infer a similar uncertainty for the intensity ratios R_{23}. The dependence of the experimental R_{23} ratio versus angle φ is shown in Fig. 6 by full squares. The obtained R_{23} values have statistical errors of ± 0.1, as provided by the least-squares fitting program, which, in fact, cover also the uncertainties related to the slight deviations of the hyperfine field distributions mentioned above. However, in order to avoid the influence of the hyperfine field distributions on the determination of the R_{23} ratios, and considering the fact that the $P(B_{hf})$ distributions must be independent

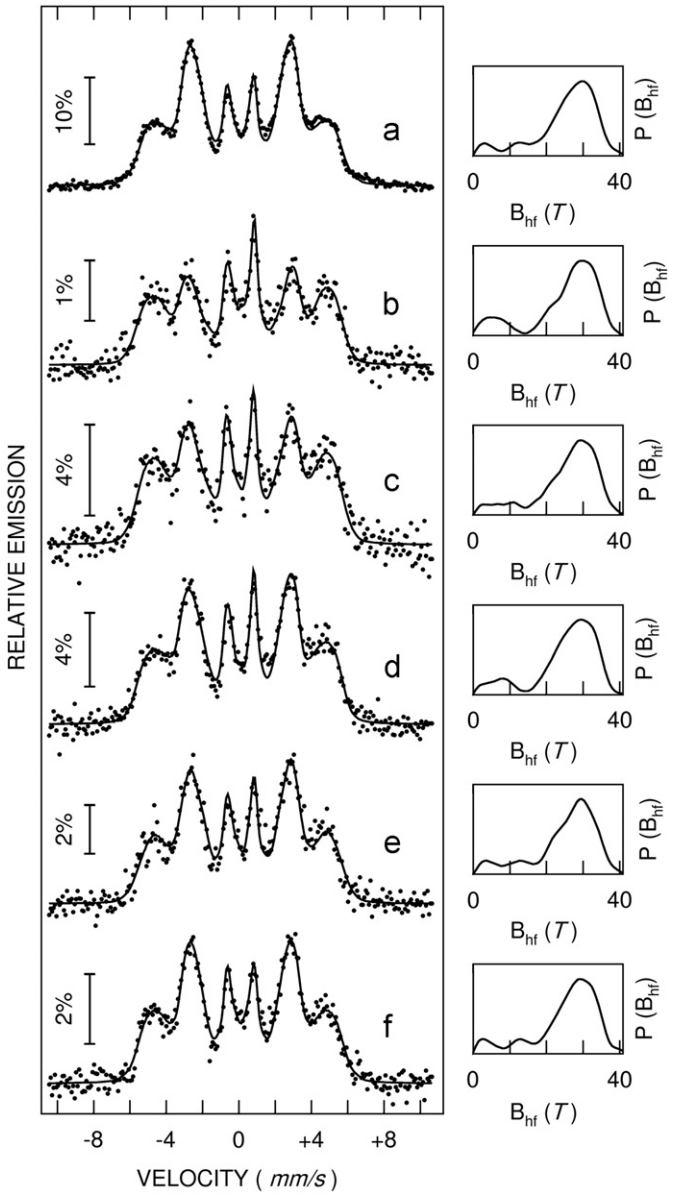

Fig. 5. Conversion electron Mössbauer spectra collected at room temperature and at magnetic remanence on a Fe(Cu) thin film grown on a Si(0 0 1) substrate carrying a Cu buffer layer. The following geometries were chosen: perpendicular geometry ($\Phi=90^\circ$) (a), and non-perpendicular geometry with $\Phi=50^\circ$ and $\varphi=-30^\circ$ (b), 0° (c), 30° (d), 60° (e) and 90° (f) (φ is the angle between a reference direction and the in-plane projection of the γ-ray direction). Right hand side: corresponding hyperfine field distributions, $P(B_{hf})$.

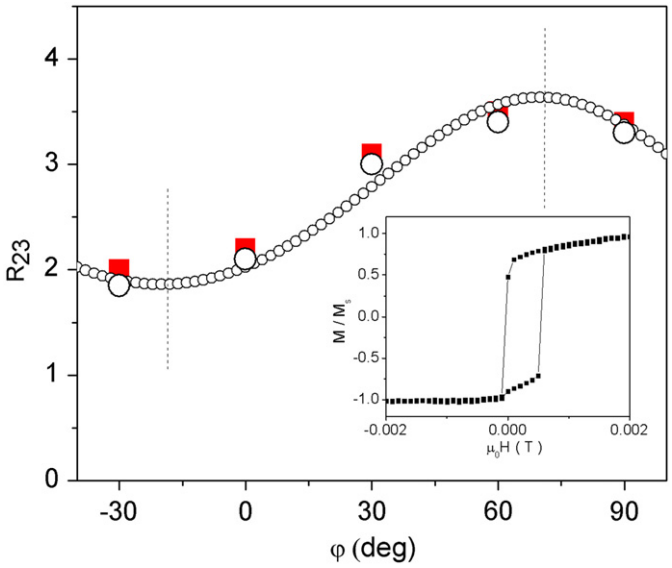

Fig. 6. Experimentally obtained R_{23} ratios for a fitting procedure (Fig. 5) with free hyperfine field distributions $P(B_{hf})$ (full squares), and for a fitting procedure (Fig. 7) with the hyperfine field distribution in perpendicular geometry ($\Phi=90^\circ$) (Fig. 5(a)) imposed to be the same for all spectra in non-perpendicular geometry ($\Phi=50^\circ$) (open large circles). Also shown is the theoretical fit curve $R_{23}(\varphi)$ according to Eqs. (2) and (4) with $\Phi=50^\circ$ and $\varphi'=35^\circ$ (small open circles). Inset: longitudinal MOKE loop measured with the in-plane external field applied along to the [1 1 0] direction of the Si(0 0 1) substrate.

of the spin orientation, a new (independent) least-squares fitting was performed on the spectra obtained in non-perpendicular geometry (Fig. 5(b)–(f)), imposing in all those cases the same reference hyperfine field distribution that was obtained in perpendicular geometry (Fig. 5(a)) for the in-plane oriented spins. The result of the latter fitting procedure is shown in Fig. 7. One can notice that this fitting is of the same quality as that shown in Fig. 5(b)–(f). The as-obtained values of the intensity ratio R_{23}, which differ just slightly from the previous ones, are also plotted in Fig. 6 (open large circles). Both of these experimental series of data are well fit by the theoretical set of Eqs. (2) and (4) within the following conditions: $\phi=50^\circ$, $\varphi'=35(5)^\circ$ and the center φ_0 of the angular spin distribution shifted by $\varphi=-20^\circ$ from the marked direction at $\varphi=0^\circ$ (see the theoretical fit curve as small open circles in Fig. 6). Physically the reason for an angular spin distribution in the Fe(Cu) film in the remanent state is related to the presence of magnetic domains extended over Fe(Cu) crystallites with angular distributed easy axes. The single-crystalline nature of the Si substrate is partially transferred via the Cu buffer layer to the Fe(Cu) film, which consequently will acquire a magnetic texture, with a preferred orientation of the magnetic hyperfine fields (and, hence, of the Fe spins) along a certain direction in the sample plane (the [1 1 0] direction of the Si(0 0 1) substrate in our case). It is worth mentioning that the 2-nm thick Fe film is too thin to prove its crystallographic texture by X-ray diffraction. However, the Mössbauer spectroscopical result is also qualitatively supported by the longitudinal magneto-optical Kerr effect (MOKE). The MOKE hysteresis loop (shown in the inset of Fig. 6) measured with the in-plane external magnetic field applied along the [1 1 0] direction of the Si(0 0 1) substrate exhibits a nearly rectangular shape, which is typical for a loop taken along the magnetic easy axis. This observation provides support for the Mössbauer result, indicating the existence of a magnetic texture with the average orientation of the magnetic easy axes along the [1 1 0] direction of the Si(0 0 1) substrate. In addition, the low value of the coercive field (less than 5 Oe) sustains the lack of oxidation of the Fe film.

Finally, in the second case (ii), when the angular spin distribution is modified by an external factor (e.g., an external magnetic field), the problem can be completely solved only if at least one of the two parameters, which define the model distribution, can be provided by a complementary experimental method. For example, in the case of an exchange-spring bilayer with an epitaxially grown hard layer and uniaxial in-plane magnetic anisotropy [2], the angular spin distribution in the soft magnetic layer, under the influence of the applied field, can be obtained by taking Mössbauer spectra with the easy axis of the hard layer parallel to the field and perpendicular to the in-plane projection of the γ-ray direction (i.e., along the *Oy* axis, Fig. 1). The step-shape angular spin distribution may be characterized in this situation by

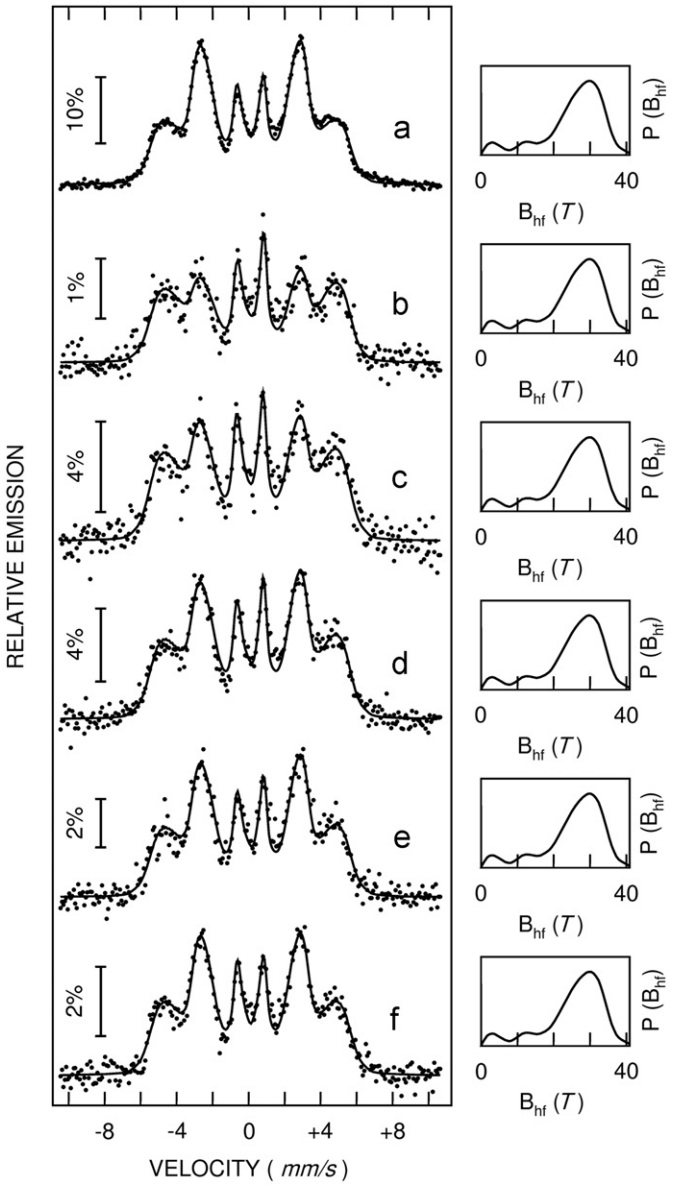

Fig. 7. Same conversion electron Mössbauer spectra as shown in Fig. 5, but least-squares fitted in a different way: the hyperfine field distribution $P(B_{hf})$ in perpendicular geometry ($\Phi=90^\circ$) (Fig. 5(a) and Fig. 7(a)) is imposed to all spectra in non-perpendicular geometry ($\Phi=50^\circ$) (Fig. 7(b)–(f)). The fittings are of the same quality as in Fig. 5.

angles φ_1 (where the probability jumps from 0 to P_0) and φ_2 (where the probability jumps back from P_0 to 0). According to Fig. 2, the connections to the previous parameters are $\varphi_2-\varphi_1=\Delta\varphi=2\varphi'$ and $\varphi_2+\varphi_1=2\varphi_0$, and Eq. (4) can be straightforwardly expressed by the new parameters φ_1 and φ_2. This time the sample cannot be rotated in its own plane (the field would act along another internal magnetic direction and not along the easy axis of the hard magnet) and the distribution aperture $\varphi_2-\varphi_1$ can be uniquely determined only via the knowledge of φ_1 [2].

Acknowledgments

This work was granted by the Romanian National Authority for Scientific Research through Contract CNCSIS-PCCE ID_76 and PN09-450103. In part supported by Deutsche Forschungsgemeinschaft (SFB 491). We thank M. Przybylski (Halle) for critically reading our article. W.K. is grateful to J. Kirschner for stimulating discussions and for his hospitality in Halle/Saale.

References

[1] E.E. Fullerton, J.S. Jiang, M. Grimsditch, C.H. Sowers, S.D. Bader, Phys. Rev. B 58 (1988) 12193.
[2] V.E. Kuncser, M. Doi, W. Keune, M. Askin, H. Spies, J.S. Jiang, A. Inomata, S.D. Bader, Phys. Rev. B 68 (2003) 064416.
[3] F. Radu, H. Zabel, Exchange Bias Effect of Ferro-/Antiferromagnetic Heterostructures, Springer Tracts in Modern Physics, vol. 227, Springer, Berlin, 2007, p. 97.
[4] F. Stromberg, W. Keune, V.E. Kuncser, K. Westerholt, Phys. Rev. B 72 (2005) 064440.
[5] S. Zhang, P.M. Levy, A. Fert, Phys. Rev. B 45 (1992) 8689.
[6] M. Johnson (Ed.), Magnetoelectronics, Elsevier, Amsterdam, 2004.
[7] K.V. O'Donovan, J.A. Borchers, C.F. Majkrzak, O. Hellwig, E.E. Fullerton, Phys. Rev. Lett. 88 (2002) 67201.
[8] H.L. Meyerheim, J.-M. Tonnerre, L. Sandratskii, H.C.N. Tolentino, M. Przybylski, Y. Gabi, F. Yildiz, X.L. Fu, E. Bontempi, S. Grenier, J. Kirschner, Phys. Rev. Lett. 103 (2009) 267202.
[9] R. Röhlsberger, H. Thomas, K. Schlage, E. Burkel, O. Leupold, R. Rüffer, Phys. Rev. Lett. 89 (2002) 23720.
[10] T. Klein, R. Röhlsberger, O. Crisan, K. Schlage, E. Burkel, Thin Solid Films 51 (2006) 52531.
[11] W.A.A. Macedo, B. Sahoo, J. Eisenmenger, M.D. Martins, W. Keune, V. Kuncser, R. Röhlsberger, O. Leupold, R. Rüffer, J. Noguès, K. Kai Liu, Schlage, Ivan K. Schuller, Phys. Rev. B 78 (2008) 224401.
[12] W.A.A. Macedo, S. Sahoo, V. Kuncser, J. Eisenmenger, I. Felner, J. Noguès, W. Kai Liu, Keune, Ivan K. Schuller, Phys. Rev. B 70 (2004) 224414.
[13] V. Kuncser, W. Keune, M. Vopsaroiu, P.R. Bissell, Nucl. Instrum. Meth. Phys. Res. B 196 (2002) 135.
[14] V. Kuncser, W. Keune, M. Vopsaroiu, P.R. Bissell, Nucl. Instrum. Meth. Phys. Res. B 245 (2006) 539.
[15] H.D. Pfannes, H. Fischer, Appl. Phys. 13 (1977) 317.
[16] J.M. Greneche, F. Varret, J. Phys. C: Solid State Phys. 15 (1982) 5333.
[17] J.M. Greneche, M. Henry, F. Varret, J. Magn. Magn. Mater. 26 (1982) 153.
[22] G. Barault, L. Rohr, J.M. Greneche, J. Magn. Magn. Mater. 128 (1993) 258.
[21] G. Le Gal, F. Varret, J. Magn. Magn. Mater. 111 (1992) 115.
[18] J.M. Greneche, F. Varret, Solid State Commun. 54 (1985) 985.
[19] F. Varret, Hyperfine Interact. 30 (1986) 135.
[20] F. Varret, J.C. Walker, C.L. Chien, J. Magn. Magn. Mater. 66 (1987) 225.
[23] J.M. Greneche, F. Varret, J. Phys. Lett. 43 (1982) L233.
[24] Q.A. Pankhurst, M.R.J. Gibbs, J. Phys. C: Condens. Matter 5 (1993) 3275.
[25] V. Kuncser, W. Keune, M. Vopsaroiu, P.R. Bissell, B. Sahoo, G. Filoti, J. Optoelectron. Adv. Mater. 5 (2003) 217.
[26] D. Liljequist, T. Ekdahl, U. Bäverstam, Nucl. Instrum. Meth. 155 (1978) 529.
[27] R.A. Brand, Nucl. Instrum., Meth. Phys. Res. 28 (1987) 417.